

## Response functions for deep inelastic scattering from $^{40}\text{Ca}$

M. Deady,\* C. F. Williamson, and J. Wong

*Department of Physics and Bates Linear Accelerator Center,  
Massachusetts Institute of Technology, Cambridge, Massachusetts 02139*

P. D. Zimmerman, C. Blatchley, J. M. Finn,<sup>†</sup> J. LeRose, and P. Sioshansi<sup>‡</sup>

*Department of Physics and Astronomy, Louisiana State University, Baton Rouge, Louisiana 70803*

R. Altemus, J. S. McCarthy, and R. R. Whitney

*Department of Physics, University of Virginia, Charlottesville, Virginia 22901*

(Received 7 March 1983)

Deep inelastic electron scattering cross sections have been measured from  $^{40}\text{Ca}$  at energies between 100 and 375 MeV and at scattering angles of  $90^\circ$  and  $140^\circ$ . Longitudinal and transverse response functions at three-vector momentum transfers of 330, 370, and 410 MeV/c were extracted from these data using a Rosenbluth separation. The integrated longitudinal response functions for the three momentum transfers are found to have, respectively, 65%, 75%, and 90% of the longitudinal strength predicted by the Fermi gas model.

[ NUCLEAR REACTIONS Deep inelastic electron scattering from  $^{40}\text{Ca}$ , extracted transverse and longitudinal response functions. ]

Deep inelastic electron scattering provides information about the behavior of the individual nucleons in the nuclear medium, a vastly different environment than the free nucleon state. Early work<sup>1</sup> in this kinematic region suggested that the gross features of the data were well explained by a process of single nucleon knockout. The target nucleus could be described by a shell model, or a Fermi gas model with the adjusted parameters of a Fermi momentum,  $k_F$ , and an average separation energy,  $\bar{\epsilon}$ . For the most part, none of these models included specific nucleon-nucleon interactions beyond the Pauli exclusion principle.

Rosenbluth separations allow the study of longitudinal (charge) and transverse (current and magnetization) components of the nuclear excitation individually. Such a separation of response functions in the deep inelastic region can contribute to the understanding of nuclear excitation mechanisms, since many of the effects that one expects to observe (such as the predominantly transverse mesonic effects) would have a particular signature in the separated response functions. In this paper separated longitudinal and transverse response functions for  $^{40}\text{Ca}$  for momentum transfers up to 410 MeV/c and energy losses up to 210 MeV are presented.

Electrons ranging in energy from 100 to 375 MeV were scattered from a natural calcium target and were observed at laboratory angles of  $90^\circ$  and  $140^\circ$  at the Bates Linear Accelerator.<sup>2</sup> The scattered electrons were momentum analyzed by the 900 MeV/c energy-loss spectrometer using the standard Bates system of multiwire proportional counters and Lucite Čerenkov detectors.<sup>3</sup> The absolute uncertainty of these measurements was of the order of 5%, and was dominated by the uncertainty in target thickness. System efficiency and normalization were determined to be constant by comparing the calculated electron-proton scattering cross section to scattering from the hydrogen in a polyethylene target. In the few cases in

which deep inelastic measurements with the same angle and electron energy were repeated, the data agreed within 2% for spectra taken as much as three years apart.

It was discovered that spectra at incident energies greater than 300 MeV contained a significant background of pions produced in the target. In order to estimate these background contributions data were taken with the polarity of the magnet reversed. A silica aerogel Čerenkov detector ( $n=1.05$ ) was substituted for the Lucite detectors ( $n=1.49$ ) in the standard Bates detector system. This aerogel allowed the rejection of slower particles, thereby leaving the spectra free of pions. Those few energies for which no data were taken with the aerogel detector were corrected by scaling the pion component of the reversed polarity spectra, using the aerogel spectra as references for the correction. The pion component of the spectrum was narrowly peaked at an energy loss slightly greater than that of the center of the quasielastic peak. Its greatest effect was 25% of the measured cross section at 370 MeV and  $90^\circ$ , and its contribution was substantially less elsewhere.

It was also found that the light collection efficiency of the Lucite detector was less than that of the aerogel detector at the lower final energies. A correction to the data collected with the Lucite counters, roughly 2% at 110 MeV and 6% at 80 MeV final electron energies, was derived from a comparison of deep inelastic data taken with the two detectors under the same experimental conditions.

A pair-produced electron background which rises sharply at final energies less than 100 MeV was eliminated by using the corresponding positron contribution in reversed polarity spectra. This correction was only important in the regions of highest energy loss and never amounted to more than 10% of the measured cross section.

An additional correction to the data was made for electrons that scattered from the target chamber aperture into the acceptance phase space of the spectrometer.<sup>4</sup> This

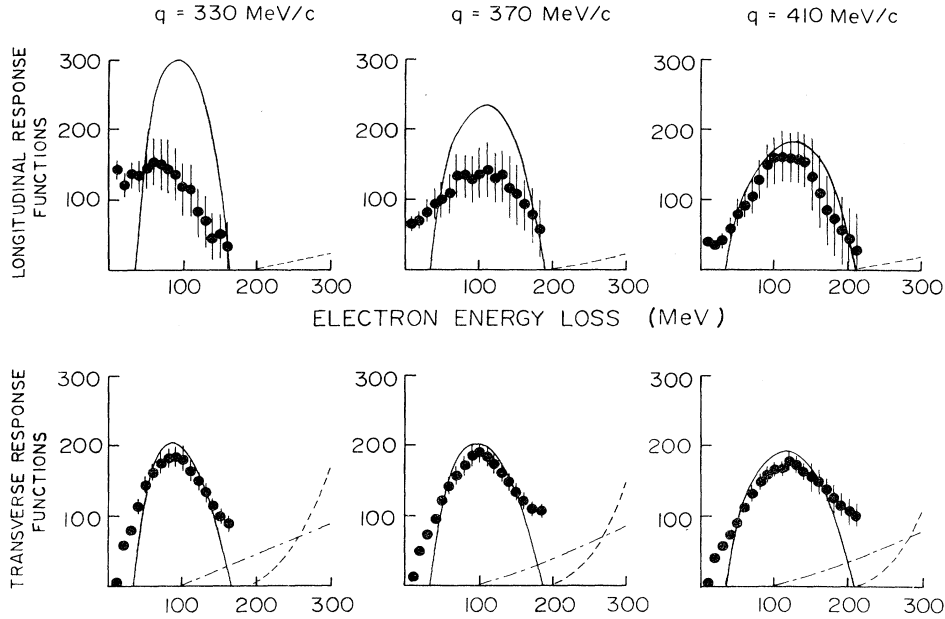


FIG. 1. Experimentally separated longitudinal and transverse response functions for  $^{40}\text{Ca}$  as a function of energy transfer for constant vector momentum transfer are shown. The error bars shown reflect the systematic errors, the statistical errors being everywhere smaller than the data points. The solid curves show relativistic Fermi gas calculations for  $S_L$  and  $S_T$  using a Fermi momentum  $k_F = 250$  MeV/c and an effective binding energy  $\bar{\epsilon} = 33$  MeV. The dashed curves represent the contribution from real and virtual pion productions, and the dashed-dotted curves show the contributions arising from meson exchange currents (Ref. 9).

correction, based on a calculation of multiple scattering and thick-target bremsstrahlung in the chamber walls, was adjusted using measurements at  $90^\circ$  comparing the original chamber aperture with a new chamber aperture in which this background had been eliminated. This correction had its greatest effect in the region with final electron energies just less than the quasielastic peak, where its application could reduce the cross section by as much as 18%. For all of the corrections outlined above, no significant angular dependence was observed.

The elastic radiative tail was calculated according to the "exact" first Born formalism of Mo and Tsai<sup>5</sup> which includes both internal and external bremsstrahlung. This contribution is significant only at final electron energies

less than 100 MeV and is less than 20% of the measured cross section for the highest incident energies at  $90^\circ$ , and less than 10% of the measured cross section at  $140^\circ$ .

These corrected inelastic cross sections were then radiatively unfolded according to the method of Miller<sup>6</sup> to obtain the corrected inelastic double differential cross sections. The response functions at constant vector momentum transfer were extracted by interpolation<sup>7</sup> from the double differential cross sections which were measured at constant bombarding energy and scattering angle. These corrected response functions at different laboratory angles were then used to effect the Rosenbluth separations according to the formula<sup>8</sup>

$$\frac{d^2\sigma}{d\Omega d\omega} = \frac{4\pi}{M_T} \sigma_{\text{Mott}} \left\{ \left[ \frac{q_\mu^2}{q^2} \right]^2 S_L(q, \omega) + \left[ \frac{1}{2} \left[ \frac{q_\mu^2}{q^2} \right] + \tan^2 \left[ \frac{\theta}{2} \right] \right] S_T(q, \omega) \right\}.$$

In this equation  $q_\mu$  is the four-momentum transfer;  $q$  is the three-momentum transfer;  $\Omega$  is the solid angle;  $\omega$  is the energy transfer;  $\theta$  is the laboratory scattering angle;  $M_T$  is the target mass;  $\sigma_{\text{Mott}}$  is the Mott cross section; and  $S_L(q, \omega)$  and  $S_T(q, \omega)$  are, respectively, the longitudinal and transverse response functions.

The limiting factors used in determining the usable kinematic region for the separations are as follows: No final energies less than 80 MeV were used because of the detector inefficiencies and uncertainties in background subtractions. Only  $(q, \omega)$  values for a given angle were included for which there were three nearby data points at

different incident energies that could be used for interpolation. Finally, small extrapolations (less than 5% of the total  $\omega$  range) from the spectra at constant incident energy were allowed. Throughout the analysis, systematic and statistical errors were treated separately, and both types are reported.

The experimental results for the measured longitudinal and transverse response functions at three different values of  $q$  are shown in Fig. 1. Also shown are curves representing calculations for the response functions in the relativistic Fermi gas model of Van Orden.<sup>9</sup> The values used for the Fermi momentum and the average separation energy

TABLE I. Integrated experimental longitudinal strength,  $\Sigma_L$ , and its ratio to predictions of a relativistic Fermi gas model,  $R_F$  (Ref. 9).

$q$ (MeV/c)	$\omega_{\text{cutoff}}$ (MeV)	$\Sigma_L \times 10^{-4}$ <sup>a</sup>	$R_F$ <sup>a</sup>
330	160	$1.79 \pm 0.03 \pm 0.50$	$0.65 \pm 0.01 \pm 0.18$
370	180	$1.93 \pm 0.03 \pm 0.56$	$0.75 \pm 0.01 \pm 0.22$
410	210	$2.07 \pm 0.04 \pm 0.71$	$0.90 \pm 0.02 \pm 0.31$

<sup>a</sup>The first reported error represents the statistical uncertainty; the second, the estimate of systematic uncertainty.

( $k_F = 250$  MeV/c and  $\bar{\epsilon} = 33$  MeV) were characteristic of past parametrized fits to  $^{40}\text{Ca}$  data.<sup>1</sup>

As a measurement of the agreement between the data and the calculation, the longitudinal response function has been integrated for both the experimental and theoretical results. A sum of this sort should be largely independent of the choice of initial and final nuclear wave functions,<sup>10</sup> and provides a simple way to compare the agreement over a large range of inelasticity. The values of the integrated longitudinal strengths and their ratios to the theoretical integrated strengths are given in Table I. The experimental sum was taken from  $\omega = 0$  to an energy loss,  $\omega_{\text{cutoff}}$ , beyond which no separations were possible. For the two highest momentum transfers, an extrapolation was performed to a point at which the response function might be zero, based on data at lower final energies. When these extrapolations were included in the experimental sum, the observed fraction of the Fermi gas integral increased to 0.79 at  $q = 370$  MeV/c and 0.92 at  $q = 410$  MeV/c.

The treatment of the systematic errors in this analysis has been conservative; subsequent statistical analysis may reduce the size of the error envelope. Such an analysis would not, however, change the values of the data themselves. The rather large errors associated with the longitudinal response functions follow from the fact that even at  $90^\circ$ , the most forward angle used in the present work, the data are dominated by the transverse cross sections.

The contribution of various nuclear structure and dynamical effects can be estimated by a study of the individual response functions. For the longitudinal response function at the lowest momentum transfer of 330 MeV/c, there is considerable strength in the low- $\omega$  region, compared to the prediction for nucleon knockout. An enhancement of the response in this kinematic region could be evidence for non-Pauli long-range correlations in the nucleus, as, for example, collective modes of nuclear excitation.

The agreement of both the differential and integrated longitudinal strength with the Fermi gas calculations improves as the momentum transfer increases. This is a reasonable result since the impulse approximation is expected to be valid only for large momentum transfers. However, even at  $q = 410$  MeV/c, the measured strength is somewhat less than the calculated strength. The effects of short-range correlations have been investigated by Celenza *et al.*,<sup>11</sup> and modification of the nucleon effective mass and moment has been discussed by Noble.<sup>12</sup> Both of these approaches can produce reductions in the longitudinal response functions.

A comparison of the  $S_T(q, \omega)$  and the relativistic Fermi

gas calculation reveals a different pattern of agreement than for  $S_L(q, \omega)$ . There is little evidence of strength in the low- $\omega$  regions seen in the low- $q$  measurements of  $S_L(q, \omega)$ , and the agreement between the measured and calculated  $S_T(q, \omega)$  at the peak of the quasielastic scattering is as good as can be expected from such a simple model. Van Orden<sup>9</sup> estimated the contribution to the response functions from real and virtual pion currents, and the results of these calculations are shown in Fig. 1. These effects contribute mainly to the transverse response and mainly at energy losses greater than the quasielastic peak.

The previously published results for  $^{56}\text{Fe}$  (Ref. 13) differ from these results in two significant ways; for iron, a greater reduction of the longitudinal strength had been found, and the discrepancy with the Fermi gas prediction increased with increasing momentum transfer. The  $^{40}\text{Ca}$  analysis differs from that of  $^{56}\text{Fe}$  primarily in that corrections were made for the contribution of the chamber aperture scattering background in the raw spectra. The Ca analysis indicates that inclusion of this effect can result in an increase of the integrated longitudinal strength in Ca by as much as 25% at the highest momentum transfers.

The only other significant body of data in this kinematic region is the deep inelastic electron scattering data from  $^{12}\text{C}$ .<sup>14</sup> The  $^{12}\text{C}$  longitudinal response is qualitatively similar to that observed in  $^{40}\text{Ca}$  in the comparable kinematic domain in that the theoretical results calculated from the impulse approximation show improved agreement with the data as  $q$  is increased. There are, however, differences in detail in that the Fermi gas calculation tends to underestimate the measured transverse response function in  $^{12}\text{C}$ , whereas the converse was found for  $^{40}\text{Ca}$ .

The Rosenbluth separation technique is only strictly valid in the plane wave Born approximation. For a number of  $(q, \omega)$  points in this data set, experimental cross sections from  $160^\circ$  were also included in the analysis, and the separations based on  $90^\circ$ ,  $140^\circ$ , and  $160^\circ$  were linear to an accuracy well within the statistical errors. Coulomb distortion effects are evidently of little importance for this analysis.

The measurements of the detailed structure of  $S_L$  and  $S_T$  as a function of momentum transfer are new information. These results cannot be adequately explained by existing theories. Additional measurements over an expanded kinematic range will improve the quality of the separations as well as extend the  $q$  and  $\omega$  range of  $S_L$  and  $S_T$ . Further theoretical work is necessary, especially to understand the contributions from multinucleon processes.

The authors would like to express their indebtedness to T. W. Donnelly, E. J. Moniz, J. V. Noble, B. E. Norem, and J. W. Van Orden for many stimulating and enlightening conversations during the course of this work. They would also like to thank S. Pollock and J. E. Wise for assistance in the acquisition and reduction of the data, and the staff of the Bates Accelerator for experimental support. The Louisiana State University group was supported in part by the National Science Foundation and the Research Corporation. The Massachusetts Institute of Technology and University of Virginia groups were supported in part by the United States Department of Energy under Contract No. EY-76-C-02-3069 and DE-AS05-78ER05861, respectively.

\*Present address: Department of Physics, Mount Holyoke College, South Hadley, MA 01075.

†Present address: Department of Physics, Massachusetts Institute of Technology, Cambridge, MA 02139.

‡Present address: Spire Corporation, Bedford, MA 01730.

<sup>1</sup>G. R. Bishop *et al.*, Nucl. Phys. 54, 97 (1964); E. Moniz, Phys. Rev. 184, 1154 (1969); E. Moniz *et al.*, Phys. Rev. Lett. 26, 445 (1971); P. D. Zimmerman and M. R. Yearian, Z. Phys. A 278, 291 (1976); R. R. Whitney *et al.*, Phys. Rev. C 9, 2230 (1974).

<sup>2</sup>W. Bertozzi, J. Haimson, C. P. Sargent, and W. Turchinets, IEEE Trans. Nucl. Sci. NS-14, 191 (1967).

<sup>3</sup>W. Bertozzi *et al.*, Nucl. Instrum. Methods 141, 457 (1977).

<sup>4</sup>C. F. Williamson, Bates Internal Report 82-6, 1982.

<sup>5</sup>L. W. Mo and Y. S. Tsai, Rev. Mod. Phys. 41, 205 (1969).

<sup>6</sup>G. Miller, Stanford Linear Accelerator Center Report SLAC-PUB-848, 1971.

<sup>7</sup>M. Deady, Ph.D. thesis, Massachusetts Institute of Technology, 1981 (unpublished).

<sup>8</sup>T. W. Donnelly and J. D. Walecka, Annu. Rev. Nucl. Sci. 25, 329 (1975).

<sup>9</sup>J. W. Van Orden, Ph.D. thesis, Stanford University, 1978 (unpublished); private communication; J. W. Van Orden and T. W. Donnelly, Ann. Phys. (N.Y.) 131, 451 (1980).

<sup>10</sup>T. deForest, Nucl. Phys. A132, 305 (1969).

<sup>11</sup>L. S. Celenza, W. S. Pong, M. M. Rahman, and C. M. Shakin, Phys. Rev. C 26, 320 (1982).

<sup>12</sup>J. V. Noble, Phys. Rev. Lett. 46, 412 (1981).

<sup>13</sup>R. Altemus *et al.*, Phys. Rev. Lett. 44, 965 (1980).

<sup>14</sup>P. Barreau *et al.*, Nucl. Phys. A (to be published).